Journal of Structural Geology, Vol. 15, No. 7, pp. 939 to 942, 1993
Printed in Great Britain

0191-8141/93 $06.00+0.00

A graphical representation of coaxial plane strains and volume changes

STEFANO MAZZOLI

Geologisches Institut, ETH-Zentrum, Sonneggstrasse 5, CH-8092 Zürich, Switzerland

(*Received* 13 *August* 1992; *accepted in revised form* 25 *November* 1992)

Abstract—Coaxial strain history, although not representing a common situation in rocks, can provide the opportunity to quantify very important parameters such as the amount of volume change occurring during compaction and tectonic deformation. In the case of coaxial superposition of compaction and tectonic plane strain, a co-ordinate system is defined with the x–y plane lying parallel to bedding and the z axis normal to it, and with the x–z plane corresponding to the plane in which tectonic strain occurs. Bulk strain data are represented on a simple deformation plot with axes $1 + e_x$, $1 + e_z$ (where e_x and e_z are the finite extensions along the x and z axes of the co-ordinate system, respectively). With respect to the conventional Flinn diagram, the use of this plot for representing coaxial deformation paths brings several advantages, in that: (1) the magnitudes of the finite strains and their orientation with respect to the chosen co-ordinate system are represented; (2) the volume changes occurring during both compaction and tectonic strain are easily visualized for all the stages of progressive deformation; and (3) the transitions from the oblate to the prolate shape (and vice versa) of the finite strain ellipsoid during progressive deformation are shown continuously, without the artificial zig-zag pattern of the Flinn diagram.

INTRODUCTION

COAXIAL strain history is likely to represent an uncommon situation in most rocks deformed by natural tectonic processes. However, regions of coaxial strain within more complex tectonic structures are sometimes found (e.g. Reks & Gray 1982, 1983). Such areas assume a particular interest in that the simple strain geometry here makes it possible to quantify important parameters such as the volume changes preceding (i.e due to compaction) and/or accompanying tectonic deformation (e.g. Oertel 1970, Beutner & Charles 1985, Wright & Henderson 1992). Different methods may be employed for the graphical representation of such deformation (e.g. Flinn 1962, Hsu 1966, Ramsay 1967, Hossack 1968, Owens 1974). On the conventional logarithmic Flinn diagram, coaxial superposition of tectonic plane strain (with or without volume change) and compaction produces a complex deformation path, where total strain moves from the oblate to the prolate field and back to the oblate field during deformation (Ramsay & Wood 1973, Sanderson 1976, Ramsay & Huber 1983). In the present paper, a simple deformation plot is discussed that can conveniently represent strain and volume changes occurring by this type of deformation sequence.

DEFORMATION PLOT

Since the deformations considered in the present study are all symmetric relative to bedding, a co-ordinate system is conveniently defined with respect to bedding. The chosen system has z normal to bedding and the x–y plane lying parallel to the layering (Fig. 1a). The finite extensions along the x, y and z axes of the co-ordinate reference frame are indicated as e_x, e_y and e_z, respectively. They are distinguished from the principal extensions of the finite strain ellipsoid ($e_1 \geq e_2 \geq e_3$), which can assume different orientations with respect to the co-ordinate system.

Compaction is here treated as a simple gravitational loading producing a volume loss Δ_0 (Ramsay & Wood 1973). It results in a uniaxial strain with only one non-zero principal extension, a shortening ($e_3 < 0$) parallel to the z axis. Tectonic strain occurs in the x–z plane, and can itself be accompanied by an incremental volume change Δ_i (Ramsay & Wood 1973). No stretch occurs along the y axis of the co-ordinate reference frame throughout the whole deformation ($e_y = 0$). Under these conditions, the three-dimensional deformation can be described by means of a two-dimensional plot having the axial lengths $1 + e_x$ as abscissa and $1 + e_z$ as ordinate.

The lines with equations $1 + e_x = 1 + e_z$, $1 + e_x = 1$ and $1 + e_z = 1$ divide the positive quadrant into six fields, each of them characterized by a different orientation of the principal axes of the finite strain ellipsoid ($X \geq Y \geq Z$) with respect to the co-ordinate reference frame (Fig. 1b). The features of the finite strain ellipsoid within the six different fields are summarized in Table 1.

Fields 1 and 6 contain finite strain ellipsoids which have $e_3 = 0$, and positive e_1, e_2. These ellipsoids lie completely outside the original unit sphere from which they were derived, and clearly have a positive dilatation Δ. Ellipsoids in fields 3 and 4 have $e_1 = 0$, and negative e_2, e_3; they show negative dilatations, and lie completely inside the unit sphere. Ellipsoids in fields 2 and 5 have $e_2 = 0$, e_1 positive and e_3 negative, and can show either positive or negative dilatations. The fields of positive and negative dilatation can be determined from the equation $(1 + e_1)(1 + e_2)(1 + e_3) = 1 + \Delta$ (Ramsay 1967, p. 123). For $e_2 = 0$, we have $(1 + e_1)(1 + e_3) = 1 + \Delta$. In fields 2 and 5, this equation is equivalent to: $(1 + e_x)(1 + e_z) = 1 + \Delta$ (cf. Table 1). Ellipsoids with positive dilatation ($\Delta > 0$) plot in the field $(1 + e_x)(1 + e_z) > 1$,

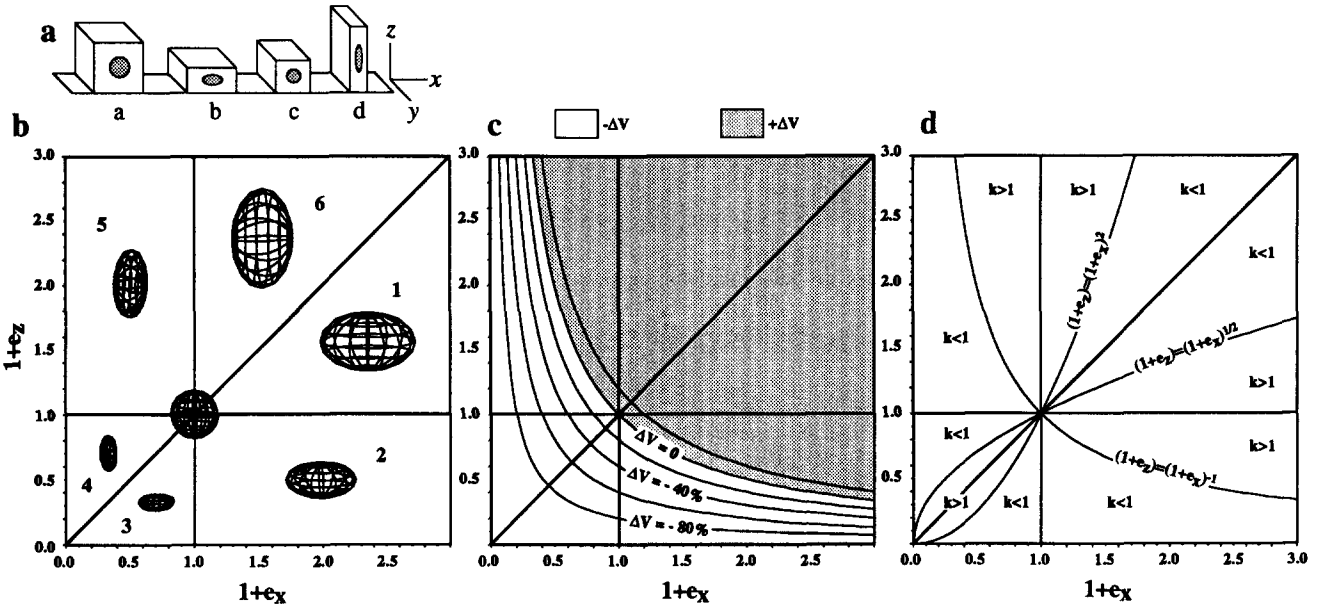

Fig. 1. (a) Some stages of the deformation sequence considered in the text: a = initial stage; b = after compaction; c and d = progressive tectonic coaxial plane strain. Co-ordinate reference frame is shown. No stretch occurs along the y axis of the co-ordinate system during the whole deformation sequence ($e_y = 0$). (b) The six deformation fields defined by the lines of equations $1 + e_x = 1 + e_z$, $1 + e_x = 1$ and $1 + e_z = 1$ (e_x and e_z are the finite extensions along the x and z axes of the co-ordinate system, respectively). The deformation ellipsoid for each of the six fields is schematically represented. The features of the finite strain ellipsoids within the six different fields are summarized in Table 1. (c) Fields of positive and negative dilatations and curves of percent volume change (ΔV). Fields of prolate ($k > 1$) and oblate ($k < 1$) strain.

those with negative dilatation ($\Delta < 0$) plot in the field $(1 + e_x)(1 + e_z) < 1$ (Fig. 1c). Different ellipsoids having the same Δ value will plot on a curve of the form: $(1 + e_z)(1 + e_x) = 1 + \Delta$. This equation can be used to generate a series of curves of constant Δ, which define the amount of volume dilatation involved during compactional and/or tectonic deformation (Fig. 1c).

The fields of prolate and oblate strain ellipsoids can also be defined in the diagram. Prolate strain is defined by the conditions $k > 1$, where: $k = (R_{XY} - 1)/(R_{YZ} - 1)$, $R_{XY} = (1 + e_1)/(1 + e_2)$, and $R_{YZ} = (1 + e_2)/(1 + e_3)$ (Flinn 1962). Using the relations in Table 1, the equations for prolate strain in terms of the plot axes $(1 + e_x, 1 + e_z)$ can be obtained:

$$\text{fields 1 and 4:} \quad 1 + e_z < (1 + e_x)^{1/2}$$

$$\text{fields 2 and 5:} \quad 1 + e_z > (1 + e_x)^{-1}$$

$$\text{fields 3 and 6:} \quad 1 + e_z > (1 + e_x)^2.$$

In the same way, the equations for oblate strain ($k < 1$) are given by:

$$\text{fields 1 and 4:} \quad 1 + e_z > (1 + e_x)^{1/2}$$

$$\text{fields 2 and 5:} \quad 1 + e_z < (1 + e_x)^{-1}$$

$$\text{fields 3 and 6:} \quad 1 + e_z < (1 + e_x)^2.$$

These equations define six different fields, alternatively characterized by prolate and oblate strain (Fig. 1d). These fields can be represented in the same deformation plot together with the curves of constant Δ and the six fields defining magnitude and orientation of the principal strains to give the final form of the diagram (Fig. 2a). The lines with equation $1 + e_x = 1 + e_z$, $1 + e_x = 1$ and $1 + e_z = 1$, which define fields 1–6, also represent positions of uniaxial (prolate or oblate) strain.

In a deformation sequence of the type considered here (Fig. 1a) prolate and oblate strains result from the effect of volume changes preceding and/or accompanying plane strain. Therefore, prolate and oblate strain states are not directly comparable to true constriction and flattening (e.g. Ramsay & Wood 1973).

Table 1. Main features of finite strain ellipsoid in the six fields of Fig. 1(b). $e_1 > e_2 > e_3$ are the principal extensions of the finite strain ellipsoid; e_x, e_y, e_z, are the finite extensions along the x, y and z axis of the co-ordinate system, respectively

Field	Values of e	Axes of the finite strain ellipsoid	Axes of the co-ordinate reference frame
1	$e_1 = e_x > 0$	X	parallel to x
	$e_2 = e_z > 0$	Y	parallel to z
	$e_3 = e_y = 0$	Z	parallel to y
2	$e_1 = e_x > 0$	X	parallel to x
	$e_2 = e_y = 0$	Y	parallel to y
	$e_3 = e_z < 0$	Z	parallel to z
3	$e_1 = e_y = 0$	X	parallel to y
	$e_2 = e_x < 0$	Y	parallel to x
	$e_3 = e_x < 0$	Z	parallel to z
4	$e_1 = e_y = 0$	X	parallel to y
	$e_2 = e_z < 0$	Y	parallel to z
	$e_3 = e_x < 0$	Z	parallel to x
5	$e_1 = e_z > 0$	X	parallel to z
	$e_2 = e_y = 0$	Y	parallel to y
	$e_3 = e_x < 0$	Z	parallel to x
6	$e_1 = e_z > 0$	X	parallel to z
	$e_2 = e_x > 0$	Y	parallel to x
	$e_3 = e_x = 0$	Z	parallel to y

DISCUSSION

An ideal deformation path on the $1 + e_x$ vs $1 + e_z$ diagram is first shown by means of forward modelling. Consider an argillaceous sediment undergoing compaction with a 55% volume loss ($\Delta_0 = -0.55$), followed by a tectonic plane strain involving shortening along the x axis and stretching along the z axis of our co-ordinate system. Tectonic strain is also accompanied by an incremental volume loss Δ_i occurring by displacements along the x axis (representing the shortening direction). The deformation path for this example is shown by means of both the deformation plot presented in this paper (Fig. 2a) and the logarithmic Flinn deformation plot having ln R_{YZ} as abscissa and ln R_{XY} as ordinate (Fig. 2b). During compaction, the deformation in Fig. 2(a) proceeds along the vertical line with equation $1 + e_x = 1$ from the point (1,1) to the point (1, 1 − 0.55) and is represented by a uniaxially oblate spheroid. On application of tectonic plane strain increments it enters field 3 and is characterized by: $e_1 = 0, e_2 < 0, e_3 < 0$, X parallel to y, Y parallel to x and Z parallel to z (Table 1). As deformation proceeds, the path crosses the curve of equation $1 + e_z = (1 + e_x)^2$ and enters the prolate field. When the uniaxial prolate state is reached ($1 + e_x = 1 + e_z$), the minimum (Z) and the intermediate (Y) axes of the finite strain ellipsoid interchange their positions and the deformation enters field 4. The deformation path returns to the oblate field when it crosses the curve of equation $1 + e_z = (1 + e_x)^{1/2}$. When the uniaxial oblate state is reached again ($1 + e_x = 1$) there is a new change over in the positions of the principal strain axes. The long (X) axis of the finite strain ellipsoid becomes parallel to the z axis of the reference frame and the deformation enters field 5, where it will remain for any further deformation increment of the same type. By comparing Figs. 2(a) & (b), the advantages of the simple $1 + e_x$ vs $1 + e_z$ deformation plot can be appreciated. The deformation path in Fig. 2(a) can be continuously followed into the different fields of oblate and prolate strain. Magnitude and orientation of the principal finite strain axes with respect to the reference frame (i.e. bedding) are readily obtainable for any stage of the progressive deformation. Volume changes related to both compactional and tectonic deformation are also clearly represented on this plot, whereas they cannot be visualized in Fig. 2(b). In fact, Ramsay & Wood (1973) were able to represent volume changes on the conventional logarithmic deformation plot by adding a series of lines (parallel to $K = 1$) with equation ln R_{XY} = ln R_{YZ} + ln $(1 + \Delta)$. However, such a volume-change overlay is not applicable to a deformation sequence of the type considered here, in which the path moves from the oblate to the prolate field and back to the oblate field (cf. fig. 7 in Ramsay & Wood 1973; see also Flinn 1978).

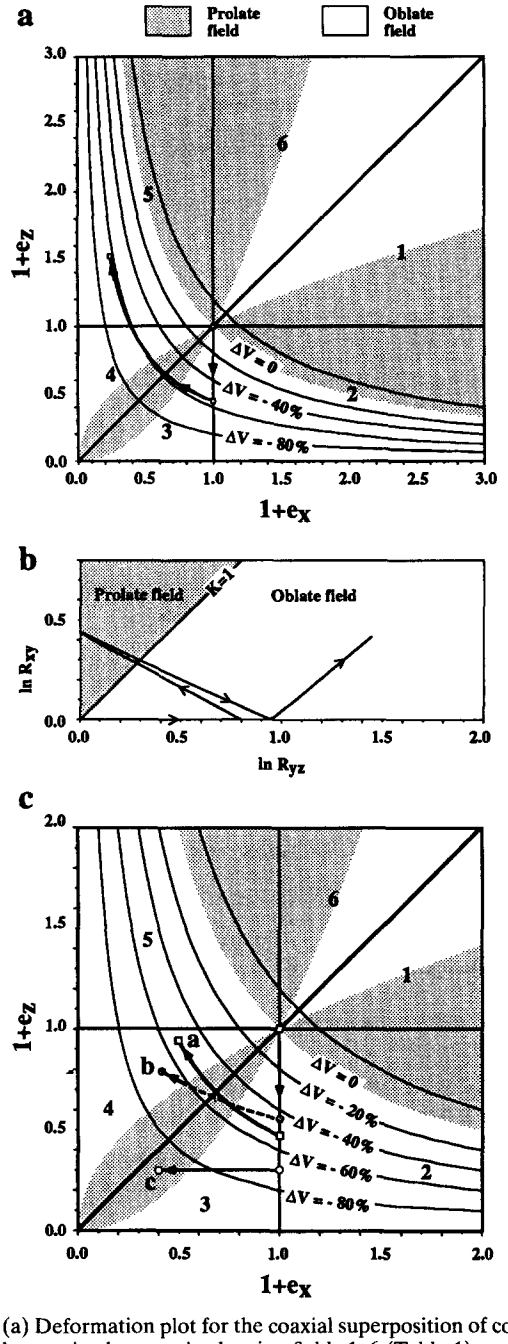

Fig. 2. (a) Deformation plot for the coaxial superposition of compaction and tectonic plane strain showing fields 1–6 (Table 1), curves of percent volume change (ΔV) and fields of prolate and oblate strain. Also shown is the deformation path resulting from the superposition of tectonic plane strain (accompanied by incremental volume loss occurring by displacements along the x axis) on a 55% vertical compaction. Note how the deformation path crosses the curves of percent volume change (ΔV) due to the effect of volume change during tectonic deformation. (b) Logarithmic deformation plot for the same deformation as in (a). (c) Three different natural deformation paths on the $1 + e_x$ vs $1 + e_z$ plot: a = superposition of compaction and plane strain not accompanied by volume change (data from Oertel 1970); b = superposition of compaction and plane strain accompanied by volume change (data from Beutner & Charles 1985); c = superposition of compaction and tectonic deformation occurring exclusively by volume change (data from Wright & Henderson 1992).

Three different types of possible deformation sequences will be now discussed using finite strain data from naturally deformed rocks.

(a) *Superposition of compaction and plane strain not accompanied by volume change*

Oertel (1970) was able to decompose the observed strain in a sample of lapillar tuff from the English Lake district into a compaction component and a tectonic component. He found a 53% compaction ($\Delta_0 = -0.53$)

and a tectonic plane strain of 2:1:0.5 ($\Delta_i = 0$), with an approximately coaxial geometry of superposition (cf. Sanderson 1976). Pre-tectonic (compactional) deformation plots on the vertical line of equation $1 + e_x = 1$ at the point (1, 1 − 0.53). Since calculated tectonic strain occurs at constant volume ($\Delta_i = 0$), the deformation path for tectonic deformation is parallel to the curves of percent volume change in the diagram (Fig. 2c, path a). Total finite strain resulting from the superposition is strongly oblate, with a maximum extension parallel to the y axis of the co-ordiniate system (field 4, Table 1).

(b) *Superposition of compaction and plane strain accompanied by volume change*

Beutner & Charles (1985), using both the shape of reduction spots and conodont extensions, described a coaxial superposition of compaction and plane strain accompanied by large volume loss in the hinge zones of near-isoclinal folds in red slates from the Hamburg sequence, Pennsylvania. Mean total finite strain resulted from the superposition of a tectonic deformation of 1.41:1:0.41 ($\Delta_i = -0.42$) on a 44% compaction. The deformation path (b in Fig. 2c), constructed assuming that volume loss during tectonic deformation occurred at constant rate, crosses in this case the curves of percent volume change. The final state plots again in field 4, and is of oblate type.

(c) *Superposition of compaction and tectonic deformation occurring exclusively by volume change*

Considerable amount of volume loss associated with pressure solution accompanying slaty cleavage formation has been shown by Wright & Henderson (1992) in Cambrian–Ordovician flysch sediments from Nova Scotia. Mean total finite strain recorded from fold hinge regions of coaxial deformation consists of a 60% tectonic shortening occurring entirely by volume loss, which was preceded by a 70% diagenetic compaction. The deformation path is in this case particularly simple, consisting of a vertical volume reduction due to compaction and of a tectonic shortening along the $1 + e_x$ axis not compensated by any extension in other directions (Fig. 2c, path c). The total finite strain is strongly prolate, with a maximum stretch parallel to the y axis of the co-ordinate system and a vertical minimum extension (field 3, Table 1).

CONCLUSIONS

In rocks where coaxial superposition of tectonic plane strain (with or without volume change) and compaction can be documented, bulk strain data can be conveniently represented on a $1 + e_x$ vs $1 + e_z$ diagram (Fig. 2a). If additional information about the volume changes occurring during tectonic deformation is also available, the whole deformation path can be reconstructed.

The simple $1 + e_x$ vs $1 + e_z$ deformation plot allows a complete description of the deformation, in that it shows:

(1) the orientation of the axes of the finite strain ellipsoid with respect to the co-ordinate system;

(2) the magnitude of the principal strains;

(3) the (prolate or oblate) shape of the finite strain ellipsoid;

(4) the volume changes involved in the compaction and in the tectonic deformation.

Acknowledgements—I am grateful to John Ramsay, Dorothee Dietrich, Giorgio Pennacchioni, Mary Ford and Neil Mancktelow for critical reading of the manuscript and for their useful comments and suggestions. Reviews by Richard Lisle and Jack Henderson helped to improve the manuscript. Financial support from the ETH Zürich is gratefully acknowledged.

REFERENCES

Beutner, E. C. & Charles, E. G. 1985. Large volume-loss during cleavage formation, Hamburg sequence, Pennsylvania. *Geology* **13**, 803–805.

Flinn, D. 1962. On folding during three-dimensional progressive deformation. *Q. J. geol. Soc. Lond.* **118**, 385–433.

Flinn D. 1978. Construction and computation of three-dimensional progressive deformation. *J. geol. Soc. Lond.* **135**, 291–305.

Hossack, J. R. 1968. Pebble deformation and thrusting in the Bygdin area (Southern Norway). *Tectonophysics* **5**, 315–334.

Hsu, T. C. 1966. The characteristics of coaxial and noncoaxial strain paths. *J. Strain Anal.* **1**, 216–222.

Oertel, G. 1970. Deformation of a slaty lapillar tuff in the English Lake District. *Bull. geol. Soc. Am.* **78**, 1173–1187.

Owens, W. H. 1974. Representation of finite strain state by three axis planar diagrams. *Bull. geol. Soc. Am.* **86**, 307–310.

Ramsay, J. G. 1967. *Folding and Fracturing of Rocks*. McGraw-Hill, New York.

Ramsay, J. G. & Huber, M. I. 1983. *The Techniques of Modern Structural Geology, Volume* 1: *Strain Analysis*. Academic Press, London.

Ramsay, J. G. & Wood, D. S. 1973. The geometric effects of volume change during deformation processes. *Tectonophysics* **16**, 263–277.

Reks, I. J. & Gray, D. R. 1982. Pencil structure and strain in weakly deformed mudstone and siltstone. *J. Struct Geol.* **4**, 161–176.

Reks, I. J. & Gray, D. R. 1983. Strain patterns and shortening in a folded thrust sheet: an example from the southern Appalachians. *Tectonophysics* **93**, 99–128.

Sanderson, D. J. 1976. The superposition of compaction and plane strain. *Tectonophysics* **30**, 35–54.

Wright, T. O. & Henderson, J. R. 1992. Volume loss during cleavage formation in the Meguma Group, Nova Scotia, Canada. *J. Struct. Geol.* **14**, 281–290.